Embedded Self Organizing Systems (Vol. 12. No. 14. 2025) (pp.14-20)

Embedded Selforganizing Systems

Issue Topic: "Artificial Intelligence Based Applications in Engineering Science"

A Study on Lung Cancer Detection Using Deep Learning

Daariimaa Chuluunbaatar
Mongolian University of Science and Technology
Ulaanbaatar, Mongolia
chdaariimaa@must.edu.mn

Uranchimeg Tudevdagva
Mongolian University of Science and Technology, Citi University
Ulaanbaatar, Mongolia
uranchimeg@must.edu.mn

Ganbat Ganbaatar
Mongolian University of Science and Technology
Ulaanbaatar, Mongolia
ganbatg@must.edu.mn

***Abstract*—Lung cancer is among the leading causes of mortality worldwide, and early detection is critical to improving patient survival. Recent advances in artificial intelligence particularly deep learning-based image analysis have opened new opportunities for earlier diagnosis. This study aims to develop a deep learning model to classify four categories of lung computed tomography (CT) images (malignant and benign) and to implement it in a mobile application. We developed a hybrid convolutional architecture combining MobileNetV2 and ResNet50 and trained it on the open-access "Lung Cancer 4 Types" dataset from Kaggle. Model performance was evaluated using standard metrics, including overall accuracy, precision, recall, and F1-score. The proposed model achieved an overall accuracy of 85.4%, with per-class F1-scores ranging from 80.0% to 94.0%, indicating effective discrimination among lung cancer categories. Finally, the trained model was converted to TensorFlow Lite and integrated into an Android application, thereby bringing deep learning solutions closer to clinical practice.**

Keywords— CT images, Image Processing, Convolutional Neural Network (CNN), MobileNetV2, ResNet50, Mobile Application

I. INTRODUCTION

Cancer is a leading cause of death worldwide, accounting for nearly 10 million deaths in 2020, or almost one in six deaths. One in five people dying from cancer is due to lung cancer [1]. The lungs are a pair of primary respiration organs located in the thoracic cavity on either side of the mediastinum [2]. Lung cancer is a type of cancer that starts when abnormal cells grow in an uncontrolled way in the lungs [3]. Lung cancer is characterized by highly aggressive, rapidly metastasizing cells that are often resistant to pharmacologic therapies. In its early stages, it is frequently paucisymptomatic, rendering it a "silent" disease [4]. According to the World Health Organization, in 2022, lung cancer had the second-highest global incidence, with approximately 2.21 million cases, and was the leading cause of cancer mortality, accounting for 1.8 million deaths [1]. Approximately 80–90% of cases are associated with tobacco smoking. Lung cancer disproportionately affects men and shows the highest prevalence in Central and Eastern Europe and in East Asia [4]. It is broadly classified into two types: small cell lung cancer (SCLC) and non-small cell lung cancer (NSCLC) [3].

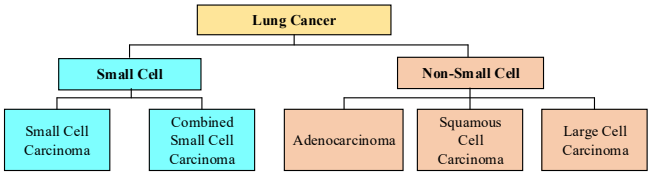

Fig. 1. Types of Lung Cancer [3]

Late-stage diagnosis and treatment delays not only incur substantial costs but also pose a significant risk to life [4].

Computed tomography (CT) scan is a key modality for early detection of lung cancer, using X-rays from multiple angles to generate detailed diagnostic images [6]. Recent advances in artificial intelligence (AI) have enabled earlier disease diagnosis by leveraging machine learning and deep learning techniques applied to large datasets collected from hospitals and healthcare institutions [7,8]. Recent studies have employed convolutional neural network (CNN) architectures to analyze lung CT images [9]. CNNs are particularly effective for deep learning tasks involving image processing and feature extraction, and are widely used to identify characteristics of lung disease [10]. This study aims to develop a mobile application for processing and classifying lung CT images to distinguish between malignant and benign conditions using deep learning methods. The dataset used in this study was obtained from Kaggle under the title "Lung Cancer 4 Types Images Dataset" [11]. It consists of CT scan images in .png and .jpg formats, categorized into four classes: Adenocarcinoma (AC), Large Cell Carcinoma (LCC), Squamous Cell Carcinoma (SCC), and Normal (benign) cells.

In contrast to previous studies that employed MobileNetV2 or ResNet50 as standalone backbones, the present work introduces the first hybrid MobileNetV2 + ResNet50 architecture trained exclusively on the Lung Cancer 4 Types dataset. The use of the hybrid architecture enabled the extraction of higher quality features from lung cancer CT images, thereby enhancing the model's overall performance

and improving its robustness. Moreover, the hybrid model is optimized for on device inference through TensorFlow Lite conversion, thereby providing a distinctive contribution for deployment in resource constrained clinical diagnostic environments. Model performance was evaluated using standard metrics, including accuracy, recall, precision, and F1-score.

II. Related work

In recent years, numerous studies in healthcare have applied image processing and machine learning (ML) and deep learning (DL) techniques. Year by year, methodologies have improved, datasets have grown, and accuracy has increased. This trend indicates that research and development in this area will continue to expand [8].

The rapid advancement of ML and DL technologies has revolutionized medical imaging, particularly in cancer detection. Among various cancer types, lung cancer has seen significant progress due to the integration of CNNs [13]. Different methods are used for the prediction of lung cancer. In the detection process, X-rays, CT, and MRI & PET scans are most used. Currently, a CT scan is the way of detecting early-stage lung cancer [14]. A CT scan uses many sequential X-ray images taken from various angles around your body and processes them to create detailed cross-sectional images (slices) of the body part [15].

TABLE I. Research studies have been conducted in the last 10 years.

№	Reference	Architecture	Dataset	Accuracy (%)
1	[16]	MobileNetV2 InceptionResNetV2, Xception	CT (LIDC-IDRI, IQ-OTH/NCCD)	99.54
2	[17]	ResNet50 VGG, Inception, Xception, BoF+Random Forest	CT (LIDC-IDRI)	95.34
3	[18]	ResNet50, VGG16 XGBoost/SVM	CT (834 CT imaging data from 396 patients)	94.3
4	[19]	ResNet50 3D-ResU-Net (seg)	CT (LIDC-IDRI)	87.3
5	[20]	ResNet50 ResNet-101, EfficientNet-B3	CT (LIDC-IDRI)	~94
6	[21]	MobileNetV2 (+U-Net)	CT (Medical Segmentation Decathlon (MSD))	87.93
7	[22]	MobileNetV3 Small and ResNet50 (Hybrid)	CT (LIDC-IDRI, IQ-OTH/NCCD)	99.38

As shown in Table I, the LIDC–IDRI dataset has been among the most widely used resources. Researchers continue to improve results by integrating additional models and refining pipelines, thereby achieving incremental performance gains. The Lung Image Database Consortium image collection (LIDC–IDRI) is an open-access repository available from the National Cancer Institute website [23]. It comprises thoracic CT scans acquired for diagnostic assessment and lung cancer screening, and includes annotated pulmonary nodules. In this study, we employ the open-access "LungCancer4Types" dataset available on Kaggle. This dataset supports four class classification of lung images. Previous studies that employed this dataset are summarized in Table II.

TABLE II. Studies using the "Lung Cancer 4 Types" dataset.

Reference	Architecture	Accuracy (%)
Santanu Roy, Shweta Singh, etc (2025) "MSAD-Net: Multiscale and Spatial Attention-based Dense Network for Lung Cancer Classification" (+ "IQ-OTH/NCCD lung cancer dataset) [24]	DenseNet-121 InceptionV3 MobileNetV2 ResNet50 ResNet-152 Xception	DenseNet-121 – 84.1; InceptionV3 – 94.4; MobileNetV2 – 85.4; ResNet50 – 80.6; ResNet-152 – 94.4; Xception – 93.8
Mohammad Q. Shatnawi, Qusai Abuein, Romesaa Al-Quraan (2024) "Deep learning-based approach to diagnose lung cancer using CT-scan images" (+ Chest CT-Scan Images Dataset) [25]	Enhanced CNN ConvNeXtSmall VGG16 ResNet50 InceptionV3 EfficientNetB0	Enhanced CNN - 100; VGG16 - 99; EfficientNetB0 - 97.9; ResNet50 - 94.5; ConvNeXtSmall - 87; InceptionV3 - 76.9

As shown in the Table II, previous studies trained various individual architectures on the "Lung Cancer 4 Types" dataset and reported their respective performance outcomes. In contrast, our study employs a hybrid training architecture on the same dataset, which has not yet been explored in prior work and therefore represents a notable novelty of this research.

III. Materials and Methods

A concise overview of the study's dataset and the applied deep learning methods is included.

A. Dataset

The dataset used in this study was obtained from Kaggle under the title "Lung Cancer 4 Types Images Dataset" [23]. This dataset provides a balanced framework for developing and evaluating machine learning and deep learning models, offering visual examples that highlight the differences between malignant lung cancer types and normal lung tissue.

(A) Adenocarcinoma

(B) Large cell carcinoma

(C) Squamous Cell Carcinoma

(D) Normal

Fig. 2. CT Images of the lung disease categories analyzed in this study [23].

As such, it is widely used as a benchmark resource for studies in computer aided diagnosis (CAD), deep learning, and medical imaging applications.

It consists of CT scan images in .png and .jpg formats, categorized into four classes: Adenocarcinoma (AC), Large Cell Carcinoma (LCC), Squamous Cell Carcinoma (SCC), and Normal (benign) cells. These images are split into 613 number of training, 72 validation and 315 testing samples. The number of training images in the AC, LCC, normal, and SCC classes are 195, 115, 148, and 155 respectively [23]. Hence, there is slight class imbalance problem, additionally, the number of total training images are too less, that is 613 images.

The "Lung Cancer 4 Types" dataset exhibits class imbalance, which increases the risk of overfitting. Consequently, previous studies that utilized this dataset often incorporated additional datasets to compensate for the imbalance and improve overall performance. In contrast, our work does not rely on supplementary datasets; instead, we employ a hybrid architecture. A hybrid architecture integrates the complementary strengths of two or more CNN backbones, enabling it to partially mitigate the limitations caused by class imbalance.

B. MobileNetV2

MobileNetV2 is a state of the art CNN architecture designed specifically for mobile and resource constrained environments. This architecture is particularly efficient due to its innovative use of depthwise separable convolutions and inverted residuals with linear bottlenecks, which significantly reduce the number of parameters and computational cost while maintaining high accuracy. This makes it particularly suitable for applications in medical imaging, where computational efficiency is critical.

Key components of MobileNetV2:

Despite being primarily designed for lightweight image classification, MobileNetV2's efficient architecture and reliance on generalizable visual features make it particularly suited for histopathological image analysis. This approach enhances the model's capability to capture subtle inter class variations, which are often difficult to discern in medical images. MobileNetV2 introduces several key architectural innovations:

1) Depthwise Separable Convolutions

This operation splits the standard convolution into two layers: a depth wise convolution that filters input channels independently, and a pointwise convolution that combines these filtered outputs to create new features. The depth wise separable convolution can be expressed as:

$$y_{i,j,k} = \sum_{m=1}^{M} \sum_{n=1}^{N} x_{i+m-1,j+n-1,k} \cdot \omega_{m,n,k} \quad (1)$$

where $y_{i,j,k}$ is the output feature map, $x_{i,j,k}$ is the input feature map, $\omega_{m,n,k}$ represents the depthwise convolution kernel, and M and N are the kernel dimensions.

Following this, the pointwise convolution is applied as:

$$z_{i,j} = \sum_{k=1}^{K} y_{i,j,k} \cdot p_k \quad (2)$$

where $z_{i,j}$ represents the final output after pointwise convolution, and p_k are the weights applied during this operation.

TABLE III. MOBILENETV2-BASED MODEL ARCHITECTURE

Layer	Type	Output shape
1	Input Layer	(224, 224, 3)
2	MobileNetV2 (Base Model)	(7, 7, 1280)
3	GlobalAveragePooling2D	(1280)
4	Batch Normalization	(1280)
5	Dense (ReLU)	(256)
6	Dropout (0.45)	(256)
7	Dense (Softmax, classes=4)	(4)

2) Inverted Residuals and Linear Bottlenecks

MobileNetV2 utilizes inverted residuals where the input and output are thin bottleneck layers, and intermediate layers are expanded. The linear bottlenecks prevent the loss of information that could occur due to non-linearities like ReLU. The operation can be described as:

$$y = \max(0, W_{exp} \cdot x) \cdot W_{proj} \quad (3)$$

Here, W_{exp} represents the expansion matrix, x is the input tensor, and W_{proj} is the projection matrix. This formulation ensures that the linear bottleneck minimizes the loss of information while maintaining computational efficiency.

3) ReLU6 Activation Function

To prevent information loss in low precision computation, MobileNetV2 employs the ReLU6 activation function, defined as:

$$ReLU6(x) = \min(\max(0, x), 6) \quad (4)$$

This bounded activation helps to reduce quantization error during low bit precision computation, making MobileNetV2 more suitable for mobile and embedded systems [14,26,27].

C. ResNet50

In 2015, Microsoft Research introduced the Residual Neural Network (ResNet) architecture to solve the issue of disappearing gradients in deep neural networks. ResNet50 is a specific variation of the ResNet architecture that uses shortcut connections called residual connections. The model uses identity mappings to add shortcut connections between layers, facilitating efficient backpropagation and improving model convergence. Therefore, a ResNet model with 50 layers is referred to as ResNet50 [24,25].

TABLE IV. RESNET50-BASED MODEL ARCHITECTURE

Layer	Type	Output shape
1	Input Layer	(224, 224, 3)
2	ResNet50 (Base Model)	(7, 7, 2048)
3	GlobalAveragePooling2D	(2048)
4	Batch Normalization	(2048)
5	Dense (ReLU)	(256)
6	Dropout (0.45)	(256)
7	Dense (Softmax, classes=4)	(4)

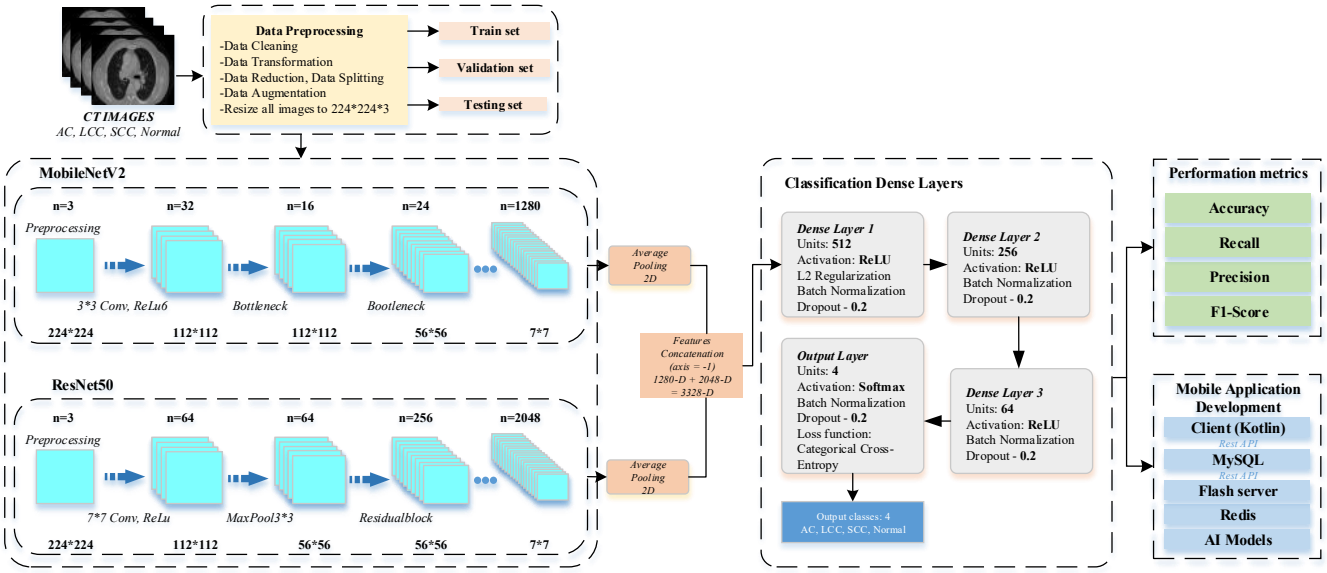

Fig. 3. Block diagram of the proposed model

D. Data Preprocessing and Augmentation

Before model training, the following preprocessing steps were performed:

- ***Data Cleaning:*** Corrupted and duplicate images were removed.
- ***Data Transformation:*** Image formats were standardized, and color channels were unified.
- ***Data Splitting:*** The dataset was partitioned into training, validation, and test subsets.
- ***Data Augmentation:*** Given the limited size of the Lung Cancer 4 Types dataset (613 training images) and the inherent challenges such as low luminance LCC samples and high inter class similarity between AC and SCC, data augmentation was employed to enrich the visual diversity of the training set and reduce overfitting.

During the preprocessing stage, the following augmentation strategies were applied:

- ✓ *Resizing:* Images were resized to a fixed dimension of 224×224 pixels to enhance computational efficiency.
- ✓ *Rotation:* Images were rotated 180°, enabling the model to classify correctly even when images are inverted.
- ✓ *Zoom:* Images were zoomed in by 15%, allowing the model to better recognize lesions of varying scales.
- ✓ *Horizontal Flip:* Images were flipped horizontally to improve the model's ability to detect lesions appearing in different orientations.
- ✓ *Vertical Flip:* Images were flipped vertically to enhance the model's capability to reliably identify lung diseases.
- ✓ *Rescale:* Pixel values were normalized to the range of 0–1, enabling the model to learn stable features and reducing the risk of overfitting.
- ✓ *Gaussian noise ($\mu = 0, \sigma^2 = 0.05$):* Effectively increased the variability of the limited dataset, helping to mitigate overfitting while improving the model's robustness and generalization, particularly for low luminance LCC images and the high visual similarity between AC and SCC.

By employing all of the aforementioned data augmentation techniques, the model was exposed to a broader range of imaging variations, thereby becoming more robust to noise and appearance changes and achieving more stable generalization to unseen CT scans.

E. Proposed Methodology

In this study, we propose a hybrid deep learning approach combining MobileNetV2 and ResNet50 for lung cancer classification from CT scan images. The block diagram of the workflow is shown in Figure 3.

The proposed workflow employs a hybrid feature extraction scheme combining MobileNetV2 + ResNet50 to enhance the representation quality of lung cancer CT images.

MobileNetV2 provides lightweight, fine grained features, while ResNet50 contributes deeper semantic representations. By processing the input CT images in parallel and applying Global Average Pooling to each branch, their outputs 1280-dimensional (MobileNetV2) and 2048-dimensional (ResNet50) vectors are concatenated into a unified 3328-dimensional feature representation.

This fused representation is processed by three fully connected layers (512, 256, and 64 units) incorporating ReLU activation, L2 regularization, Batch Normalization, and a 0.2 dropout rate, followed by a four class softmax classifier for AC, LCC, SCC, and Normal categories.

To address the limited dataset size, low luminance LCC images, and the high structural similarity between AC and SCC, a comprehensive data augmentation pipeline rotation, zooming, flipping, rescaling, and Gaussian noise ($\mu = 0$, $\sigma^2 = 0.05$) was applied to improve robustness and reduce overfitting.

The model was trained using the Adam optimizer (learning rate 1×10^{-4}), a batch size of 16, and categorical cross entropy

loss, yielding more stable convergence and improved generalization to unseen CT scans.

F. Model Evaluation

The performance of the proposed hybrid model was assessed using standard evaluation metrics, including accuracy, recall, precision, and F1-score. These metrics are defined as follows [28]:

- Accuracy: measures the proportion of correctly classified instances.

$$Accuracy = (TP + TN) / (TP + TN + FP + FN) \quad (5)$$

- Recall: indicates the proportion of true positive predictions among actual positive cases.

$$Recall = TP/(TP + FN) \quad (6)$$

- Precision: represents the proportion of true positive predictions among all positive prediction.

$$Precision = TP / (TP + FP) \quad (7)$$

- F1-Score: is the harmonic mean of precision and recall, providing a balanced assessment.

$$F1\text{-}Score = (2 * Precision * Recall / (Precision + Recall)) \quad (8)$$

TP (true positives), TN (true negatives), FP (false positives), FN (false negatives)

In addition, confusion matrix was computed for each class to assess discriminative capability.

G. Mobile application development

The trained model was converted to the TFLite format, yielding a .tflite model artifact suitable for mobile application development. In addition to the hybrid deep learning model, the system incorporates a lightweight backend architecture designed to support real time mobile inference. The mobile application, implemented using Kotlin (using Android Studio 25.1.3), communicates with a Flask based REST API server, which manages image requests and handles the end to end inference workflow.

Upon receiving a CT image from the client, the Flask server preprocesses the input and forwards it to the deployed AI model for classification. To ensure efficient request handling and low latency communication, Redis is used as an in memory message broker and caching layer, enabling optimized model loading and faster prediction responses. The prediction results including the probabilities for AC, LCC, SCC, and Normal classes are then returned to the mobile client through the REST API.

All application data and user interaction logs are stored in a MySQL database, completing the backend service pipeline. This architecture ensures scalable, reliable, and responsive deployment of the proposed hybrid model on mobile platforms

IV. RESULTS AND DISCUSSION

A. Model Training Results

The experiments were conducted on a computer equipped with an Intel Core i5 (11th generation) processor, NVIDIA GeForce MX450 GPU, and 16 GB of RAM, within the Google Colab Pro environment using Python 3 on the Google Compute Engine backend with a T4 GPU (16 GB RAM).

The proposed hybrid MobileNetV2 + ResNet50 model achieved an overall training accuracy of 85.4% for the four class lung cancer classification task.

TABLE V. BASELINE COMPARISON TABLE

Model	Accuracy (%)	Parameters (M)	Inference time (ms/image)
MobileNetV2	73.9%	3.4	14
ResNet50	80.1%	25.6	40
Hybrid (MobileNetV2 + ResNet50)	**85.4%**	**29.0**	**36**

As shown in Table V, MobileNetV2 achieved an accuracy of 73.9% with 3.4M parameters and the fastest inference time of 14 ms per image, whereas ResNet50 reached 80.1% accuracy with a substantially larger parameter count of 25.6M and an inference time of 40 ms. The proposed Hybrid (MobileNetV2 + ResNet50) model outperformed both baselines, attaining an accuracy of 85.4%, representing an improvement of 11.5 percentage points over MobileNetV2 and 5.3 percentage points over ResNet50. Despite integrating both backbones, the hybrid model required only 29.0M parameters and maintained a faster inference speed (36 ms) compared to ResNet50. These results demonstrate that the hybrid architecture provides a favorable balance between computational cost and predictive performance, offering measurable advantages over the individual backbone networks.

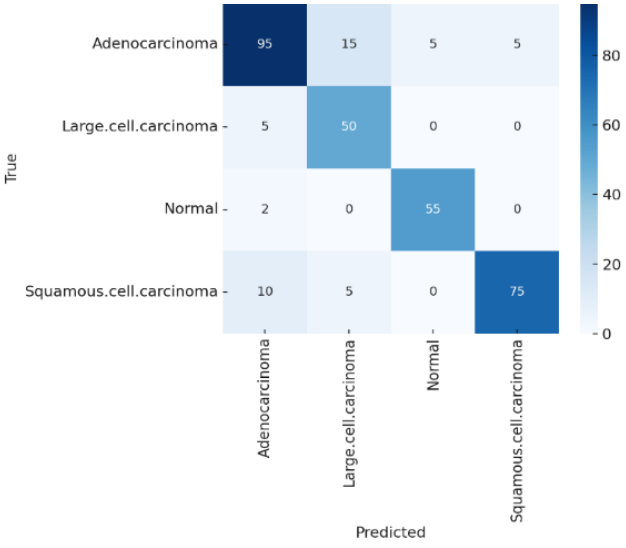

Fig. 4. Confusion matrix of CT image classification using the hybrid model

The confusion matrix in Figure 4 provides a detailed visualization of class wise prediction behavior. The model demonstrated strong performance in identifying Normal samples, achieving the highest recall of 96.5%, which indicates reliable discrimination of benign CT images.

Squamous Cell Carcinoma was also classified with high precision (93.8%) and competitive recall (83.3%), reflecting effective recognition of its characteristic radiological patterns.

TABLE VI. PERFORMANCE EVALUATION MEASURES

Class	Precision (%)	Recall (%)	F1-score (%)
Adenocarcinoma	84.8	79.2	81.9
Large Cell Carcinoma	71.4	90.9	80.0
Normal	91.7	96.5	94.0
Squamous Cell Carcinoma	93.8	83.3	88.2

Adenocarcinoma and Large Cell Carcinoma exhibited comparatively higher misclassification rates, consistent with their known visual similarity in CT imaging and the moderate class imbalance within the dataset. Adenocarcinoma achieved a precision of 84.8% and a recall of 79.2%, while Large Cell Carcinoma obtained the lowest precision (71.4%) but a relatively high recall (90.9%), indicating that although the model frequently detects LCC cases, it tends to confuse them with other malignant subtypes.

F1-scores ranged from 80.0% to 94.0% across the four classes, demonstrating balanced predictive performance. Normal images achieved the highest F1-score (94.0%), followed by Squamous Cell Carcinoma (88.2%), Adenocarcinoma (81.9%), and Large Cell Carcinoma (80.0%).

Overall, the results indicate that the hybrid feature extraction strategy yields robust and generalizable performance, particularly in distinguishing benign from malignant tissue, while certain morphological similarities among malignant subtypes remain challenging.

B. Mobile Application Development

The Android based mobile application was developed to classify lung CT images into three lung cancer subtypes and one normal lung category.

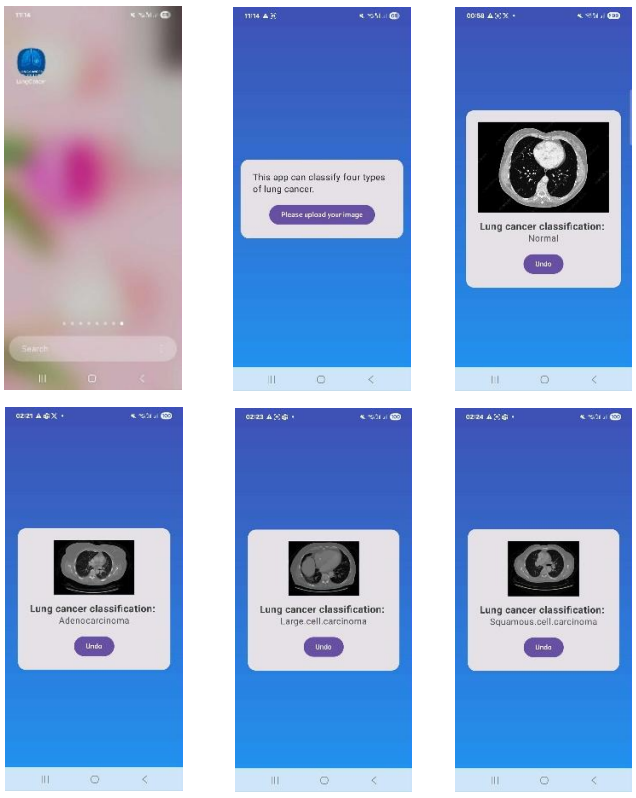

Fig. 5. User interface of the lung disease classification application

The proposed hybrid MobileNetV2 + ResNet50 model was deployed on a Samsung Galaxy S23 device to evaluate its real world on device performance.

The TensorFlow Lite version of the model has a size of 27 MB, making it suitable for mobile deployment without excessive memory usage. On device inference benchmarking yielded an average latency of 36 ms per image, corresponding to approximately 27-28 FPS, which is sufficient for near real time CT scan analysis.

This integrated architecture ensures efficient end-to-end operation, enabling accurate, responsive, and mobile-friendly lung cancer classification in real clinical environments.

Key advantages and features:

- Capable of distinguishing four lung cancer categories (Adenocarcinoma, Large Cell Carcinoma, Squamous Cell Carcinoma, and Normal).
- The trained model is integrated with a database to structure and manage data.
- The application allows users to select an image from device storage and proceed through the analysis workflow.
- The input image is fed to the trained model, which predicts the corresponding lung disease class.
- The predicted class label of one of the four categories is displayed on the application interface.

V. CONCLUSION AND FUTURE SCOPE

This study presented a hybrid deep learning approach integrating MobileNetV2 and ResNet50 to classify four lung CT image categories from the “Lung Cancer 4 Types” dataset. The proposed architecture demonstrated improved discriminative performance compared with standalone backbone models, achieving an overall accuracy of 85.4% and balanced per class F1-scores ranging from 80.0% to 94.0%.

Moreover, the conversion of the trained model to TensorFlow Lite and its deployment on a Samsung Galaxy S23 device (average latency: 36 ms; model size: 27 MB) confirmed its suitability for mobile based clinical decision support. These findings highlight the potential of lightweight hybrid architectures for real time, resource constrained diagnostic environments. Despite these encouraging results, several opportunities remain for advancing clinical applicability.

Future work should prioritize expanding the dataset, particularly for underrepresented malignant subtypes, through multi center data collection or external public repositories to reduce class imbalance and improve generalization.

To enhance interpretability, future extensions could integrate explainable AI methods such as Grad-CAM directly within the mobile application to support radiologists in understanding disease focused activation regions. Finally, alternative hybridization strategies, attention mechanisms, and transformer based encoders may further boost accuracy while maintaining computational efficiency.

ACKNOWLEDGMENT

I would like to express my sincere gratitude to Professor Uranchimeg Tudevdagva and Dr. Ganbat Ganbaatar for their professional guidance and continued support throughout this study.

REFERENCES

[1] World Health Organization, "WHO (homepage)." Online. Available: https://www.who.int/, Accessed: Sep. 26, 2025.

[2] Y. S. Khan and F. J. Carey, Histology, Lung. Treasure Island, FL, USA: StatPearls Publishing, 2025. Online. Available: https://www.ncbi.nlm.nih.gov/books

[3] World Health Organization, "Lung cancer – Fact sheet." Online. Available: https://www.who.int/news-room/fact-sheets/detail/lung-cancer, Accessed: Sep. 26, 2025.

[4] NURA Mongolia, "Lung cancer (overview)." Online. Available: https://nuramongolia.siro.mn/lung-cancer, Accessed: Sep. 26, 2025.

[5] Erdemed Clinic, "Lung cancer (clinic page)." Online. Available: https://erdemed.com/clinic/lung_cancer/, Accessed: Sep. 26, 2025.

[6] R. Javed, T. Abbas, A. H. Khan, A. Daud, A. Bukhari, and R. Alharbey, "Deep learning for lung cancer detection: a review," Artificial Intelligence Review, 2024. doi: 10.1007/s10462-024-10807.

[7] B. Hunter, S. Hindocha, and R. W. Lee, "The role of artificial intelligence in early cancer diagnosis," Cancers, vol. 14, no. 6, p. 1524, 2022. doi: 10.3390/cancers14061524.

[8] O. Elemento, C. Leslie, J. Lundin, and G. Tourassi, "Artificial intelligence in cancer research, diagnosis and therapy," Nature Reviews Cancer, vol. 21, no. 12, pp. 747–752, 2021. doi: 10.1038/s41568-021-00399-1.

[9] X. Chen et al., "Recent advances and clinical applications of deep learning in medical image analysis," Medical Image Analysis, vol. 79, 2022, Art. no. 102444. doi: 10.1016/j.media.2022.102444.

[10] R. M. Devi, R. K. Dhanaraj, S. K. Pani et al., "An improved deep convolutionary neural network for bone marrow cancer detection using image processing," Informatics in Medicine Unlocked, 2023, Art. no. 101233. doi: 10.1016/j.imu.2023.101233.

[11] Kaggle, "Search datasets/models/competitions." Online. Available: https://www.kaggle.com/search, Accessed: Sep. 26, 2025.

[12] X. Liu, K.-W. Li, R. Yang, and L.-S. Geng, "Review of deep learning based automatic segmentation for lung cancer radiotherapy," Frontiers in Oncology, vol. 11, 2021, Art. no. 717039. doi: 10.3389/fonc.2021.717039.

[13] N. T. Duc, Y.-M. Lee, J. H. Park, and B. Lee, "An ensemble deep learning for automatic prediction of papillary thyroid carcinoma using fine needle aspiration cytology," Expert Systems with Applications, vol. 188, 2022, Art. no. 115927. doi: 10.1016/j.eswa.2021.115927.

[14] R. Ochoa-Ornelas, A. Gudiño-Ochoa, J. A. García-Rodríguez, and S. Uribe-Toscano, "Enhancing early lung cancer detection with MobileNet: A comprehensive transfer learning approach," Franklin Open, 2025, Art. no. 100222. doi: 10.1016/j.fraope.2025.100222.

[15] N. Horeweg et al., "Lung cancer probability in patients with CT-detected pulmonary nodules: a prespecified analysis of data from the NELSON trial of low-dose CT screening," The Lancet Oncology, vol. 15, pp. 1332–1341, 2014. doi: 10.1016/S1470-2045(14)70389-4.

[16] S. Majumder et al., "A Mitscherlich function based ensemble of CNN models to detect lung cancer," PLOS ONE, vol. 19, no. 4, e0298527, 2024. doi: 10.1371/journal.pone.0298527.

[17] Y. K. S. Kumaran et al., "Explainable lung cancer classification with ensemble transfer learning of VGG16, ResNet50 and InceptionV3 using Grad-CAM," BMC Medical Imaging, vol. 24, 2024, Art. no. 176. doi: 10.1186/s12880-024-01345-x.

[18] W. Li et al., "Machine learning model of ResNet50-Ensemble Voting for detecting the benign and malignant nature of small pulmonary nodules," Diagnostics, vol. 13, no. 11, 2023, Art. no. 1917. doi: 10.3390/diagnostics13111917.

[19] H. Yu, J. Li, L. Zhang, Y. Cao, X. Yu, and J. Sun, "Design of lung nodules segmentation and recognition algorithm based on deep learning," BMC Bioinformatics, vol. 22, Suppl. 5, Art. no. 314, Nov. 8, 2021. doi: 10.1186/s12859-021-04234-0.

[20] M. Kanan, A. Balchandani, S. Amir Haeri, and A. S. Eesa, "AI-driven models for diagnosing and predicting outcomes in lung cancer: A systematic review," Cancers, vol. 16, no. 3, p. 674, 2024. doi: 10.3390/cancers16030674.

[21] Z. Riaz, M. Nasir, M. S. Saeed, and H. A. Habib, "Lung tumor image segmentation from CT using MobileNetV2 and transfer learning," Bioengineering, vol. 10, no. 8, p. 981, 2023. doi: 10.3390/bioengineering10080981.

[22] A. Bouamrane et al., "Toward robust lung cancer diagnosis: Integrating multiple CT datasets, curriculum learning, and explainable AI," Diagnostics, vol. 15, no. 1, p. 1, 2024. doi: 10.3390/diagnostics15010001.

[23] National Cancer Institute, "Cancer.gov (homepage)." Online. Available: https://www.cancer.gov/, Accessed: Sep. 26, 2025.

[24] S. Roy, S. Singh, P. Sahu, A. Suresh, and D. Das, "MSAD-Net: Multiscale and Spatial Attention-based Dense Network for Lung Cancer Classification," arXiv preprint arXiv:2504.14626, 2025.

[25] M. Q. Shatnawi, Q. Abuein, and R. Al-Quraan, "Deep learning-based approach to diagnose lung cancer using CT-scan images," Intelligence-Based Medicine, vol. 11, 2025, Art. no. 100188. doi: 10.1016/j.ibmed.2024.100188.

[26] K. Dong, C. Zhou, Y. Ruan, and Y. Li, "MobileNetV2 model for image classification," in Proc. 2020 2nd Int. Conf. Information Technology and Computer Application (ITCA), IEEE, Guangzhou, China, Dec. 18–20, 2020, pp. 476–480.

[27] M. Sandler, A. Howard, M. Zhu, A. Zhmoginov, and L.-C. Chen, "MobileNetV2: Inverted residuals and linear bottlenecks," in Proc. IEEE/CVF Conf. Computer Vision and Pattern Recognition (CVPR), 2018, pp. 4510–4520.

[28] A. R. Wahab Sait, "Lung cancer detection model using deep learning technique," Applied Sciences, vol. 13, no. 23, Art. no. 12510, 2023. doi: 10.3390/app132312510.